2024 IEEE 27th International Conference on
Intelligent Transportation Systems (ITSC)
September 24- 27, 2024. Edmonton, Canada

Direct Monitoring of In-situ Rail Fastener Vibrations from a Moving Train with Laser Doppler Vibrometer*

Yuanchen Zeng, *Member, IEEE*, Alfredo Núñez, *Senior Member, IEEE*, Arjen Zoeteman, Rolf Dollevoet, and Zili Li

2024 IEEE 27th International Conference on Intelligent Transportation Systems (ITSC) | 979-8-3315-0592-9/24/$31.00 ©2024 IEEE | DOI: 10.1109/ITSC58415.2024.10919662

Abstract—**Monitoring the vast number of rail fasteners across a rail network necessitates efficient monitoring technologies and autonomous data analytics. To fill the gap in direct monitoring of degraded yet unbroken rail fasteners, this paper develops a novel train-borne laser Doppler vibrometer (LDV) technology that can contactlessly measure the vibration of rail fasteners under the excitation of a moving train. Utilizing short-duration and high-sampling-rate signals measured on each fastener, a data-driven method combining clustering and statistics is developed to assess the overall behavior of fastener groups within each track section and to detect abnormal individuals. The practicality and effectiveness of this technology are demonstrated through real-world testing on an operational rail line in the Netherlands, where hundreds of rail fasteners are measured at train speeds up to 75 km/h. The train-borne LDV technology enables efficient and informative monitoring of transportation infrastructures. The developed method allows for early defect detection and both global and detailed assessments, thus facilitating condition-based maintenance.**

I. Introduction

Rail fasteners are critical components in railway infrastructures that secure rails to sleepers or track slabs and reduce the transmission of vibrations. Due to aging and train loading, rail fasteners are subject to degradation and failure. Defective rail fasteners can reduce the stability of track structures [1], deteriorate train-track dynamics [2], and cause other problems, such as rail surface defects [3]. Therefore, effective monitoring of in-situ rail fasteners is essential for the safety, quality, and sustainability of rail transportation.

As a rough estimate, there are more than 3,000 rail fasteners for every kilometer of a single railway track. Monitoring such a vast number of components across an entire rail network places high demands on the efficiency and autonomy of the technology. This is usually addressed by utilizing train-borne monitoring technologies together with data analytics methods. Machine vision technologies have been recently developed and applied to rail fastener monitoring [4]~[8]. Images of railway track surfaces at different locations along a track are taken by cameras on a moving train and then processed to detect missing and broken fasteners. Eddy current technologies are also developed and combined with machine learning methods to detect missing fasteners [9][10]. Such train-borne technologies allow large-scale monitoring of broken and missing rail fasteners for reactive maintenance purposes. However, they are unable to detect degraded fasteners that exhibit no visible geometric changes, such as reduced preload, stiffness, or damping.

Alternatively, vibration-based technologies monitor structures based on their dynamic responses [11], being effective in capturing degradation before it develops into failure [12]. In recent years, vehicle vibrations measured by accelerometers on axle boxes are used to detect defective fasteners with a spectrogram-based method [13] and a wavelet-based method [14] or to estimate rail fastening stiffness with a digital twin method [15]. Rail vibrations measured by a laser Doppler vibrometer (LDV) are used to detect missing rail fasteners with a frequency-domain method [16]. The above technologies have not yet been tested on railway tracks in operation. These technologies make use of axle box or rail vibrations to indirectly monitor rail fasteners, which can be affected by many other factors, such as wheel and track irregularities. Thus, there remains a gap in train-borne monitoring technologies that can directly measure rail fastener vibrations and assess their health conditions.

Among vibration sensing technologies, LDV is promising in filling this gap as it measures vibrations contactlessly with high sensitivity and broad bandwidth [17]. LDV is typically used to measure fixed points or along closed paths on structural surfaces [17]. Recent advancements in applying LDV on moving platforms allow vibration measurements to be made along open paths [16][18], potentially enhancing the efficiency of measurements on large-scale structures.

This paper presents a novel rail fastener monitoring technology that utilizes a train-borne LDV to directly measure rail fastener vibrations under the excitation of a moving train. This technology enables non-contact scanning of rail fasteners from a moving train under operational conditions. The technology is demonstrated with its first real-world test on an operational rail line in the Netherlands.

Based on the large volume of vibration signal segments that are of short durations and a high sampling rate, a data-driven method is further developed to assess the overall behavior of the fastener group within each track section and to detect abnormal fasteners from the normal majority. This method allows the dynamic response of rail fasteners to be characterized at both the group and individual levels.

The remainder of this paper is organized as follows. Section II presents the developed train-borne LDV technology and the field test. Section III aims to distinguish the valid signal segments for further analysis. Section IV aims to assess the fastener group in each track section and detect abnormal individuals. Section V presents the conclusions.

*Research supported by ProRail and the Europe's Rail Flagship Project IAM4RAIL (101101966) and the Dutch TKI-PPS Toeslag (TKI-HTSM.19.0172).

Yuanchen Zeng, Alfredo Núñez, Rolf Dollevoet, and Zili Li are with the Section of Railway Engineering, Delft University of Technology, Delft, 2628 CN, the Netherlands (corresponding author: Yuanchen Zeng; e-mail: Y.Zeng-2@tudelft.nl; A.A.Nunezvicencio@tudelft.nl; R.P.B.J.Dollevoet@tudelft.nl; Z.Li@tudelft.nl).

Arjen Zoeteman is with ProRail, Utrecht, 3511 EP, the Netherlands (e-mail: arjen.zoeteman@prorail.nl).

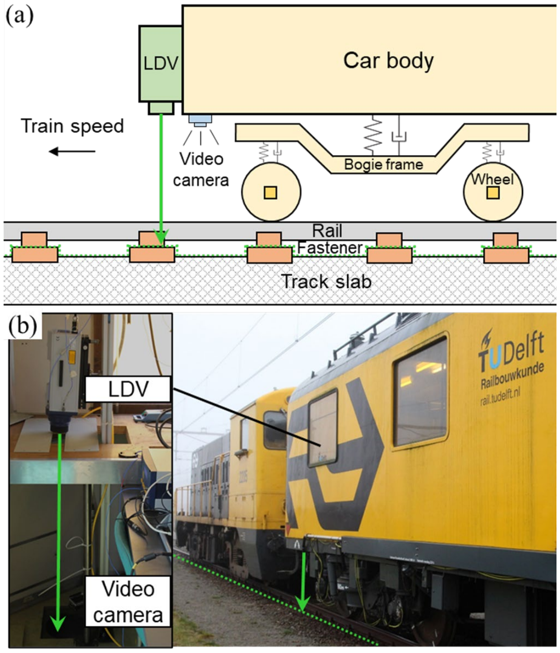

Figure 1. Train-borne LDV technology for monitoring in-situ rail fasteners. (a) System setup; (b) Implementation on the CTO train of TU Delft.

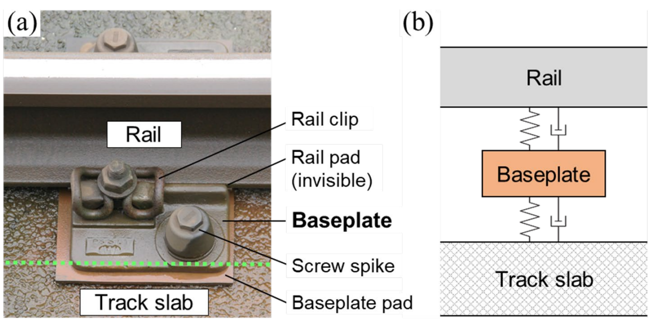

Figure 2. Rail fastening system in the case study. (a) Composition of the rail fastening system; (b) Dynamic representation.

II. Train-borne LDV Technology

A. System Setup and Implementation

Fig. 1 (a) illustrates the train-borne LDV technology for monitoring in-situ rail fasteners. A laser beam is directed from an LDV mounted on a train downwards onto rail fasteners. As the train moves, the laser spot scans rail fasteners in a row and measures their vertical vibration velocity when the laser spot is on each fastener. The trajectory of the laser spot on track structures is recorded by a video camera installed on the train.

Fig. 1 (b) shows the implementation of this technology on the CTO measurement train of TU Delft [19]. An LDV of type Polytec RSV-150 is utilized, and detailed descriptions and characteristics can be found in [20]. The sampling rate of the LDV signal is 102,400 Hz, and the frame rate of the video camera is 240 fps.

B. Targeted Rail Fastener and Field Test

In the case study presented in this paper, the rail fastening system of type 54E1 is taken as the object, as shown in Fig. 2 (a). They are used in slab track structures on bridges, viaducts, and tunnels in the Netherlands. Each fastening system consists of a baseplate made of cast steel. The baseplate is connected through clips to both sides of a rail with a rail pad placed in between. The baseplate is connected through screw spikes to track slabs with a baseplate pad placed in between. A dynamic representation of such a fastening system is further presented in Fig. 2 (b). The baseplate is the intermediate layer between the rail and the track slab, and its vibration is affected by the stiffness and damping both on top and underneath. Compared to other components, the baseplate is larger in size and has a flatter surface. Therefore, the laser spot of the train-borne LDV is targeted at the baseplates, as shown in Fig. 2 (a). By measuring the baseplate vibration, the dynamic behavior of the entire rail fastening system can be characterized.

The first field test of the developed technology was conducted on an operational rail line in Rotterdam, the Netherlands. Slab tracks on four bridges with the targeted rail fastening system are selected to showcase the measurement result, as shown in Fig. 3. The four bridges have similar slab track structures, i.e., each track slab supports six rail fasteners under a single rail. The train speed varies from 57 km/h to 75 km/h on the four bridges. A total of 343 fasteners under the left rail of the track are scanned by the train-borne LDV.

C. Signal Segmentation using Image Information

A piece of the LDV signal is shown in Fig. 4 (a) as an example. The boundaries of fasteners are determined from the video frames recorded by the camera and synchronized with the LDV signal. It can be seen that the LDV signal exhibits distinct vibration patterns within the boundaries of some fasteners, corresponding to their dynamic response measured by the LDV. Different fasteners show different amplitudes, for example, the signals on fasteners ①, ②, and ⑦ have greater amplitude than those on fasteners ③ and ⑧, reflecting their different dynamic behaviors. Meanwhile, noise is present in the LDV signal, the major source of which is the so-called speckle noise due to the continuous scanning of the laser spot on rough surfaces [18].

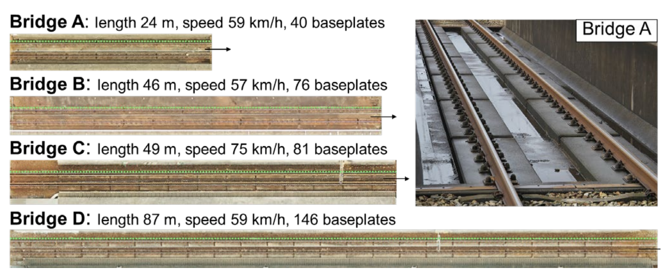

Figure 3. Selected slab track sections on four railway bridges (aerial photographs: from ProRail).

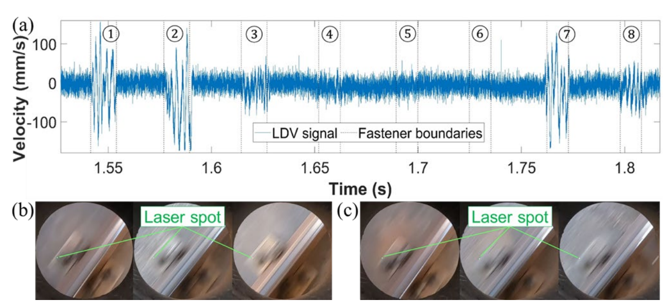

Figure 4. Signal example. (a) A piece of train-borne LDV signal measured on Bridge A; (b) Video frames when the laser spot is on a baseplate; (c) Video frames when the laser spot is not on a baseplate.

However, not all signal segments yield pronounced vibration patterns, such as ④~⑥. The major reason is that the train vibration causes the laser spot trajectory to shift laterally, which can be observed in the examples of video frames in Fig. 4 (b) and (c), corresponding to the cases when the laser spot is on and not on the surface of fasteners, respectively. Another factor that may cause this problem is the low intensity of the reflected light due to contamination on the measured surfaces. Consequently, only signal segments with vibration patterns carry valid information about the dynamics of the measured fasteners, whereas the others without vibration patterns correspond to invalid measurements on these fasteners.

The LDV signal is then cut into segments according to the boundaries of all 343 fasteners in the four selected track sections. The following section presents how to distinguish the valid signal segments for further assessment and detection.

III. Distinguishing Valid Signal Segments

In order to automatically distinguish between valid and invalid segments in the LDV signal so as to avoid manual checking and labeling, key features are extracted from each signal segment, and a clustering-based distinguishment method is developed.

A. Feature Extraction

The LDV signal segment on a rail fastener is denoted as $\{x_i\}$ (i=1, .., n), and n is the number of data points per segment. Below are the three features calculated for each signal segment, followed by the motivation for using them to distinguish the valid and invalid signal segments.

- Variation in the time domain A_{time}: Each signal segment $\{x_i\}$ is processed by a bandpass filter (with cut-off frequencies f_{L} and f_{H}) to reduce speckle noise, resulting in $\{x_{\text{B}i}\}$. The standard deviation of the filtered signal $\{x_{\text{B}i}\}$ is calculated as follows.

$$A_{\text{time}} = \sqrt{\frac{1}{n-1}\sum_{i=1}^{n}\left(x_{\text{B}i} - \frac{1}{n}\sum_{i=1}^{n}x_{\text{B}i}\right)^2}. \quad (1)$$

- Variation in the frequency domain A_{freq}: Each signal segment $\{x_i\}$ is processed by fast Fourier transform, resulting in the spectrum $\{a(f_j)\}$ (j=1, …), where $a(f_j)$ represents the amplitude at the j-th frequency f_j. The root-mean-square value of the spectrum over frequencies between f_{L} and f_{H} is calculated as follows, where M is the number of frequencies in the range.

$$A_{\text{freq}} = \sqrt{\frac{1}{M}\sum_{f_{\text{L}}<f_j<f_{\text{H}}} a\left(f_j\right)^2} \quad (2)$$

- Power spectrum density (PSD) entropy H_{psd}: This is adapted from the conventional definition of spectral entropy [13][21] to characterize the periodicity or randomness of a signal. The PSD of each signal segment $\{x_i\}$ is estimated, resulting in $\{p(f_j)\}$ (j=1, …). The PSD entropy over frequencies between f_{L} and f_{H} is calculated as follows.

$$H_{\text{psd}} = -\sum_{f_{\text{L}}<f_j<f_{\text{H}}} p\left(f_j\right)\cdot\log_2\left(p\left(f_j\right)\right). \quad (3)$$

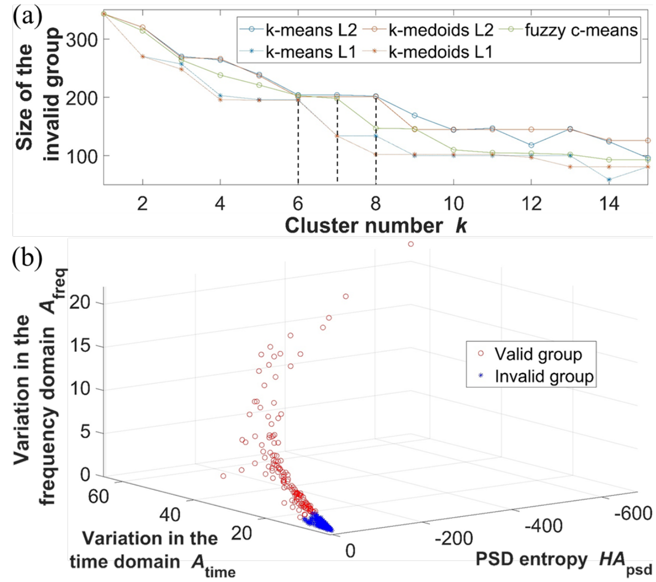

Figure 5. Clustering-based distinguishment. (a) Selection of cluster number; (b) Distinguishment result.

In general, valid segments exhibit pronounced vibration patterns in the time domain and resonance peaks in the frequency domain, whereas invalid segments are dominated by random noise in the time domain and a flat noise floor in the frequency domain. As a result, valid segments typically have larger variations in both time and frequency (larger A_{time} and A_{freq}) and higher periodicity (smaller H_{psd}), whereas invalid segments usually have smaller variations in time and frequency (smaller A_{time} and A_{freq}) and higher randomness (larger H_{psd}). The frequency range of f_{L}=200 Hz and f_{H}=800 Hz is used in this case study.

B. Clustering-based Distinguishment

Based on the three features extracted, clustering analysis is adopted in this paper to split the signal segments into two groups, valid or invalid. In case all valid signal segments have similar vibration patterns, clustering analysis with two clusters may be sufficient. However, as shown in Fig. 4 (a), significant diversity can be observed among the valid signal segments in our case study. Therefore, clustering analysis with more than two clusters is needed to separate the valid segments with different patterns into different clusters and then combine them into a single valid group, which is distinct from the remaining segments as the invalid group. Several clustering algorithms are employed and then ensembled, including k-means clustering with L2 or L1 distance, k-medoids clustering with L2 or L1 distance, and fuzzy c-means clustering with L2 distance [22].

To achieve the best distinction between the two groups, the cluster number k of each algorithm is tuned by observing its influence on the size of the group of the invalid segments. The tuning result in our case study is presented in Fig. 5 (a), in which each algorithm with a certain k is repeated 20 times to reduce the effect of random initialization. When there is only one cluster, i.e., k=1, no valid segment is distinguished. As k increases, more valid segments are distinguished while the size of the invalid group decreases. For all the different algorithms, a stable stage can be found at the size of around 200, followed by a significant drop. The cluster number k at this critical point is selected, i.e., k^*=8 for the k-means and k-medoids clustering with L2 distance, k^*=6 for the k-means and k-medoids clustering with L1 distance, and k^*=7 for the fuzzy c-means clustering.

With the selected cluster number, the clustering results of the different algorithms are obtained, in which each algorithm is repeated 50 times to reduce the effect of random initialization. These results are further ensembled by taking the majority among the five algorithms as the final label. The distinguishment result between the valid and invalid groups is shown in Fig. 5 (b). Eventually, 145 out of 343 segments are distinguished as valid. It can be seen that the segments attributed to the invalid group concentrate in the corner with small A_{time}, A_{freq}, and large H_{psd}, while the segments distinguished into the valid group (combination of various clusters) have large A_{time}, A_{freq}, and small H_{psd}. This result demonstrates the effectiveness of the feature extraction and the clustering. Meanwhile, the features of the valid segments are very diverse and dispersed in the space rather than concentrated in a single region, which reflects the rationality of using more than two clusters for the distinguishment.

IV. Assessment and Detection

Based on the distinguished valid signal segments, this section aims to monitor the health conditions of the measured rail fasteners. A statistics-based method is developed to characterize the overall behavior of the rail fasteners in each track section and to further detect the abnormal individuals from the majority.

A. Statistics of Key Features

Four key features are utilized to characterize the dynamic behavior of each rail fastener – two for the frequency of its vibration and the other two for the amplitude of its vibration.

The mean frequency of each valid signal segment within the frequency band of interest is employed as one of the frequency features of the fastener vibration. It is denoted as F_{mean} and defined based on the PSD spectrum $\{p(f_j)\}$ (j=1, …) of a signal segment as follows [23]. In other words, it is the average of frequencies weighted by the PSD.

$$F_{\mathrm{mean}} = \frac{\sum_{f_{\mathrm{L}} < f_j < f_{\mathrm{H}}} p(f_j) f_j}{\sum_{f_{\mathrm{L}} < f_j < f_{\mathrm{H}}} p(f_j)} \tag{4}$$

The median frequency of each valid signal segment within the frequency band of interest is employed as the other frequency feature of the fastener vibration. The median frequency is denoted as F_{med} and defined as follows [23]. In other words, F_{med} is the frequency that divides the spectrum into two regions with an equal sum of PSD.

$$\sum_{f_{\mathrm{L}} < f_j < F_{\mathrm{med}}} p(f_j) = \sum_{F_{\mathrm{med}} < f_j < f_{\mathrm{H}}} p(f_j) = \frac{1}{2} \sum_{f_{\mathrm{L}} < f_j < f_{\mathrm{H}}} p(f_j) \tag{5}$$

The above two frequency features are reported to be robust to noise in signals [23], thus being suitable for this case study considering the presence of significant speckle noise in the LDV signal. Additionally, the variation in the time domain A_{time}, defined in (1), and the variation in the frequency domain A_{freq}, defined in (2), are utilized as the amplitude features.

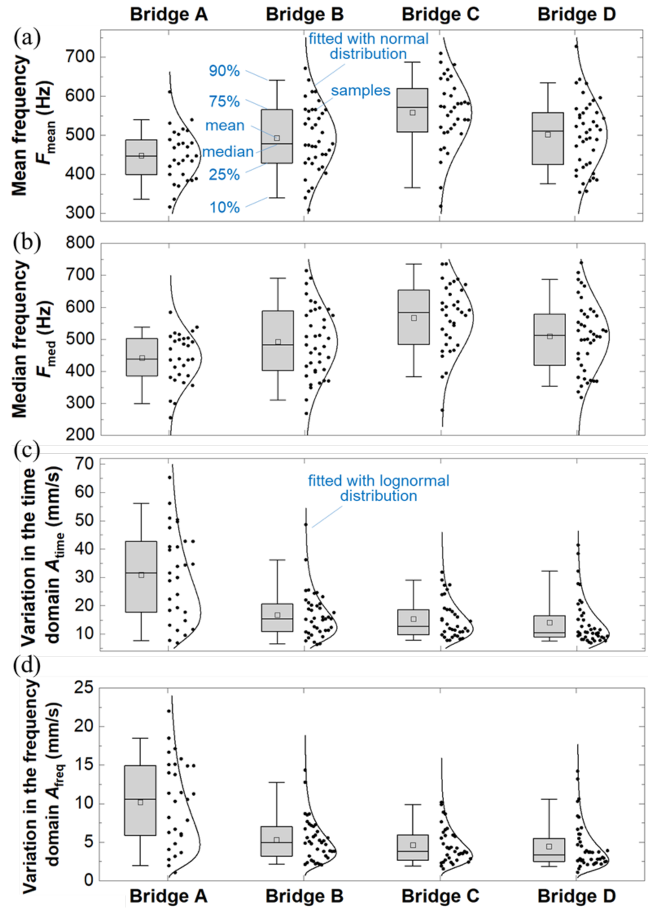

Figure 6. Statistics of key features in different track sections. (a) Mean frequency; (b) Median frequency; (c) Variation in the time domain; (d) Variation in the frequency domain.

TABLE I. Parameters of the Fitted Distributions on Different Track Sections

Features	Fasteners on Bridge A	Fasteners on Bridge B	Fasteners on Bridge C	Fasteners on Bridge D
F_{mean}	$N(448, 66^2)$	$N(492, 87^2)$	$N(558, 88^2)$	$N(502, 88^2)$
F_{med}	$N(442, 79^2)$	$N(492, 111^2)$	$N(567, 104^2)$	$N(510, 109^2)$
A_{time}	$LN(3.3, 0.63^2)$	$LN(2.7, 0.46^2)$	$LN(2.6, 0.42^2)$	$LN(2.5, 0.47^2)$
A_{freq}	$LN(2.1, 0.75^2)$	$LN(1.5, 0.50^2)$	$LN(1.4, 0.49^2)$	$LN(1.3, 0.58^2)$

The distributions of these four features for the valid signal segments measured on the four track sections are plotted in Fig. 6. For each track section, the two frequency features, F_{mean} and F_{med}, have similar statistical patterns, while the two amplitude features, A_{time} and A_{freq}, have similar statistical patterns. The samples of F_{mean} and F_{med} are effectively characterized by fitting with normal distributions, in each of which the majority is distributed around the mean in a symmetric manner with higher density closer to the mean. The samples of A_{time} and A_{freq} are effectively characterized by fitting with lognormal distributions that exhibit skewed patterns, i.e., the majority is concentrated in the small amplitude region with the amplitude of the peak density lower than the mean, whereas the long tail towards the large amplitude contains the minority. The parameters of the fitted distributions are listed in Table 1, and all the fits pass the Kolmogorov–Smirnov test [24].

B. Overall Assessment of Fastener Group

By comparing the results from the rail fasteners in the four track sections in Fig. 6 and Table 1, significant differences can be observed. Among the four sections, the rail fasteners on Bridge A have the lowest frequency features (the lowest mean and median) as well as the largest and most spread amplitude features (the largest mean, median, and standard deviation). More than half of the samples have amplitude features larger than the mean.

The rail fasteners on Bridges B~D follow similar spreading patterns in the distributions of both the frequency and amplitude features. Compared to Bridge A, their frequency features are higher (higher means and medians), and their amplitude features are less spread (smaller standard deviations). More than half of their amplitude features are smaller than the mean. The rail fasteners on Bridge C have the highest frequency features (the highest mean and median) and the most concentrated amplitude features in small amplitude regions (the smallest standard deviation).

The above results indicate the differences in the dynamic behaviors between the rail fastener groups in the four track sections. This may be caused by the use of rail fasteners from different suppliers or the different maintenance activities on the different bridges. Meanwhile, the degradation of rail fasteners due to different train-track-bridge interactions may also contribute to such differences. In general, the degradation of a rail fastener may cause a reduction in fastening stiffness and damping, thus reducing their vibration frequency and increasing their vibration amplitude. In this sense, the result of the rail fasteners on Bridge A (with the lowest frequency and the highest amplitude) indicates the most severe degradation among the four sections, whereas that on Bridge C (with the highest frequency and the second lowest but most concentrated amplitude) indicates the healthiest. Further verification is needed to confirm this assessment result.

C. Detection of Abnormal Individuals

Furthermore, the abnormal rail fasteners in each of the track sections are detected using the mean frequency F_{mean} and the variation in the time domain A_{time}. Since F_{mean} follows a normal distribution and A_{time} follows a lognormal distribution, a two-dimensional normal distribution of F_{mean} and $\ln(A_{\text{time}})$ is used to fit these two features in each of the track sections. Fig. 7 shows the fitting results, which depict the joint probability distribution of the frequency and amplitude features in each track section. The measured samples of F_{mean} and $\ln(A_{\text{time}})$ are also plotted in Fig. 7.

A slight correlation between the two features can be observed from the results of Bridge B and C, i.e., the higher the vibration frequency, the lower the vibration amplitude. Most of the measured samples are located in high-probability regions, whereas a few are located in low-probability regions. Some of these low-probability minorities have large amplitude features, as indicated by the white boxes in Fig. 7. These individuals are considered to be abnormal, while further verification is needed to confirm this detection result.

It is noteworthy that the case study in this paper focuses on rail fasteners in four short track sections on bridges. When longer track sections are considered, the vibrations of their rail fasteners may exhibit more pronounced variations, potentially affecting the effective detection of anomalies. To address this issue, a proper division strategy is recommended, which is to divide each long track section into more internally comparable groups. The division can be based on structural information of railway tracks, such as the properties of track components (e.g., the types of fasteners and sleepers) and the locations of distinct structures (e.g., level crossings, bridges, and turnouts).

The developed monitoring methodology achieves the characterization of the rail fastener response at both the group and the individual levels. This is of great value to engineering practice in view of the vast number of rail fasteners across a rail network. The overall assessment of the fastener group in each track section can provide the ranking of the health conditions of rail fasteners in different track sections so that unhealthy track sections can be prioritized for inspection and maintenance. The detection of abnormal rail fasteners in each track section can further support the detailed planning of inspection and maintenance within each track section.

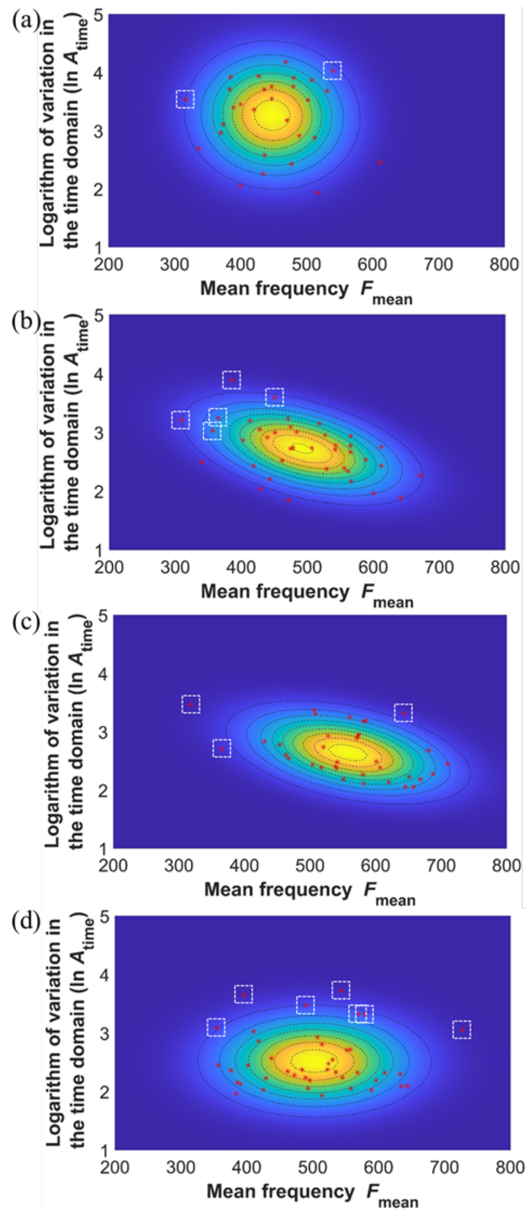

Figure 7. Detection of abnormal fasteners within different track sections. (a) Bridge A; (b) Bridge B; (c) Bridge C; (d) Bridge D.

V. Conclusion

This paper proposes a novel train-borne LDV technology for the vibration measurement of rail fasteners from a moving train and the assessment of their dynamic responses. The applicability and usability of this technology are demonstrated through the real-world test on an operational rail line. The main conclusions are summarized below.

- The valid signal segment exhibits a pronounced vibration pattern when the laser spot is on the surface of its baseplate, and the different rail fasteners have significantly different dynamic behaviors.
- The overall distributions of the frequency and amplitude features from the different groups of rail fasteners indicate their different performances in different track sections.
- The minority of rail fasteners with the low probability density and the large amplitude feature are distinguished as abnormal from the majority.

This case study focuses on a specific type of rail fastener used on the bridges, while the technology can also be applied to other fastener types. The configuration design will be improved to reduce the proportion of invalid samples due to lateral vehicle motion and to increase the adaptivity to various types of rail fasteners, thus covering as many rail fasteners as possible. The test is conducted at speeds up to 75 km/h, limited by the proximity to stations, but the setup is suitable for investigations at higher speeds. Field confirmation of the abnormal fasteners is not yet possible due to restricted access to the railway track in operation. More measurements will be conducted to expand the testing scale, particularly at higher train speeds. Further validation, such as track inspection, modal analysis, and trend analysis, will be conducted to verify the monitoring results. Our long-term goal is to apply the train-borne LDV technology to frequently monitor rail fasteners and potentially other critical components across a rail network, capture their degradation trends, and support predictive maintenance and intelligent life management of transportation infrastructures.

Acknowledgment

We thank Jan Moraal, Jurjen Hendriks, and Li Wang for their support during the field test and also thank the reviewers of this paper for their valuable comments and suggestions.

References

[1] O.V. Aharkov, V.M. Tverdomed, V.D. Boiko, V.V. Kovalchuk, and O.H. Strelko, “Influence of the structural design of rail fastenings on ensuring the stability of track gauge in operating conditions,” *IOP Conf. Ser.: Mater. Sci. Eng.*, vol. 708, no. 1, 012001, Dec. 2019.

[2] J. Li, and H. Shi, “Impact of rail fastener looseness on vertical dynamic responses of high-speed vehicle and ballastless track,” *Int. J. Struct. Stab. Dyn.*, vol. 21, no. 14, 2140006, Dec. 2021.

[3] X. Zhao, Z. Li, and R. Dollevoet. “Influence of the fastening modeling on the vehicle-track interaction at singular rail surface defects,” *J. Comput. Nonlin. Dyn.*, vol. 9, no. 3, 031002, Feb. 2014.

[4] Y. Li, H. Trinh, N. Haas, C. Otto, and S. Pankanti, “Rail component detection, optimization, and assessment for automatic rail track inspection,” *IEEE Trans. Intell. Transp. Syst.*, vol. 15, no. 2, pp. 760–770, Apr. 2014.

[5] X. Gibert, V. M. Patel, and R. Chellappa, “Robust fastener detection for autonomous visual railway track inspection,” in *2015 IEEE Winter Conference on Applications of Computer Vision*, pp. 694–701, Feb. 2015.

[6] H. Cui, J. Li, Q. Hu, and Q. Mao, “Real-time inspection system for ballast railway fasteners based on point cloud deep learning,” *IEEE Access*, vol. 8, pp. 61604–61614, Dec. 2019.

[7] J. Liu, H. Liu, C. Chakraborty, K. Yu, X. Shao, and Z. Ma, “Cascade learning embedded vision inspection of rail fastener by using a fault detection IoT vehicle,” *IEEE Internet Things J.*, vol. 10, no. 4, pp. 3006–3017, Feb. 2023.

[8] J. Liu, Y. Qiu, X. Ni, B. Shi, and H. Liu, “Fast detection of railway fastener using a new lightweight network Op-YOLOv4-Tiny,” *IEEE Trans. Intell. Transp. Syst.*, vol. 25, no. 1, pp. 133–143, Jan. 2024.

[9] P. Chandran, F. Thierry, J. Odelius, S.M. Famurewa, H. Lind, and M. Rantatalo, “Supervised machine learning approach for detecting missing clamps in rail fastening system from differential eddy current measurements,” *Appl. Sci.*, vol. 11, no. 9, 4018, Apr. 2021.

[10] P. Chandran, F. Thiery, J. Odelius, H. Lind, and M. Rantatalo, “Unsupervised machine learning for missing clamp detection from an in-service train using differential eddy current sensor,” *Sustainability*, vol. 14, no. 2, 1035, Jan. 2022.

[11] O. Avci, O. Abdeljaber, S. Kiranyaz, M. Hussein, M. Gabbouj, and D.J. Inman, “A review of vibration-based damage detection in civil structures: from traditional methods to machine learning and deep learning applications,”. *Mech. Syst. Signal Process.*, vol. 147, 107077, Jan. 2021.

[12] M. Oregui, A. Núnez, R. Dollevoet, and Z. Li, “Sensitivity analysis of railpad parameters on vertical railway track dynamics,” *J. Eng. Mech.*, vol. 143, no. 5, 04017011, Feb. 2017.

[13] X. Yin, X. Wei, and H. Zheng, “Railway track vibration analysis and intelligent recognition of fastener defects,” *Adv. Theory Simul.*, vol. 5. No. 10, 2200027, Jul. 2022.

[14] A. Vishwakarma, S.K. Singh, V. Racherla, and A. Dasgupta, “Detection of rail fastener assembly defects using axle-box acceleration,” *J. Vib. Eng. Technol.*, pp.1–21. Mar. 2024.

[15] C. Shen, P. Zhang, R. Dollevoet, A. Zoeteman, and Z. Li, “Evaluating railway track stiffness using axle box accelerations: a digital twin approach,” *Mech. Syst. Signal Process.*, vol. 204, 110730, Dec. 2023.

[16] C. Yang, K. Kaynardag, and S. Salamone, “Missing rail fastener detection based on laser Doppler vibrometer measurements,” *J. Nondestruct. Eval.*, vol. 42, no. 3, 68, Jul. 2023.

[17] P. Chiariotti, C. Rembe, P. Castellini, and M. Allen, “Laser Doppler vibrometry measurements in structural dynamics,” *Handbook of Experimental Structural Dynamics*. pp.1–45. Sep. 2020.

[18] Y. Zeng, A. Nunez, and Z. Li, “Speckle noise reduction for structural vibration measurement with laser Doppler vibrometer on moving platform,” *Mech. Syst. Signal Process.*, vol. 178, 109196, Oct. 2022.

[19] Y. Zeng, A. Nunez, and Z. Li, “Railway sleeper vibration measurement by train-borne laser Doppler vibrometer and its speed-dependent characteristics,” *Comput.-Aided Civ. Infrastruct. Eng.*, Jan. 2024.

[20] A. Dräbenstedt, J. Sauer, and C. Rembe. “Remote-sensing vibrometry at 1550 nm wavelength,” in *AIP Conference Proceedings*, vol. 1457, no. 1, pp. 113–121. Jun. 2012.

[21] Y.N. Pan, J. Chen, and X.L. Li, “Spectral entropy: a complementary index for rolling element bearing performance degradation assessment,” *Proc. Inst. Mech. Eng., Part C: J. Mechan. Eng. Sci.*, vol. 223, no. 5, pp.1223–1231. May 2009.

[22] G. Gan, C. Ma, and J. Wu, *Data Clustering: Theory, Algorithms, and Applications*. Philadelphia, PA: Society for Industrial and Applied Mathematics, 2007.

[23] A. Phinyomark, S. Thongpanja, H. Hu, P. Phukpattaranont, and C. Limsakul, “The usefulness of mean and median frequencies in electromyography analysis,” in *Computational Intelligence in Electromyography Analysis-A perspective on Current Applications and Future Challenges*, vol. 23, pp.195–220, Oct. 2012.

[24] V.W. Berger, and Y. Zhou, “Kolmogorov–Smirnov test: overview,” *Wiley StatsRef: Statistics Reference Online*, Sep. 2014.